Ultra-High Resolution PET Detector using Lead Walled Straws

Nader N. Shehad, M.E.E., Christopher S. Martin, and Jeffrey L. Lacy, Ph.D.,

Abstract— **In the last few years a high emphasis has been placed on the design and use of PET cameras for small animal studies, for example, to aid in the development of human gene therapies by imaging transgenic animals such as mice. Although, such techniques have an extraordinary potential for both clinical and basic biomedical science applications, its full realization is severely hampered by the expense, complexity and physical limitation of crystal detectors widely used in today's cameras. In particular, crystals are costly and very difficult to segment to the desired 1 mm level. Furthermore, depth of interaction error in the 1 cm or greater crystal depth required causes severe degradation of off-axis resolution. This project seeks to develop enhanced high resolution PET through the highly novel approach of the lead walled straw (LWS). In a Phase I NIH project, feasibility of application of this high energy physics spinoff technology has been proven, and in fact it has been demonstrated that considerably enhanced imaging characteristics can be achieved. A 2 mm LWS modular unit has been developed which has produced 1.0 mm FWHM axial spatial resolution. When utilized in ring arrays, such a module will produce a reconstructed volumetric spatial resolution of less than 2 μl, which is a factor of 8 improvement compared to the best commercial camera. Furthermore axial sensitive field of view can be readily extended to as large as 20 to 40 cm, and very high sensitivity can be achieved at modest cost.**

I. Introduction

HIGH resolution positron emission tomography (PET) imaging is a technique of high current interest, largely driven by research applications in small animal imaging [1], [2]. All of the systems under development are based on crystal detectors, principally LSO, and as such suffer from several drawbacks, including high cost and resolution improvement impeded by crystal segmentation and depth of interaction limitations. Lead-walled straw (LWS) detectors with a diameter of 5 mm have been previously reported by our group for use in clinical human PET applications [3]. This technology, which conceptually draws from straws used in high energy physics (HEP) applications, carries signiÞcant advantages including lower cost, larger geometric acceptance, and greatly improved spatial resolution. The aims of the current research were development and performance testing of smaller 2 mm diameter LWS detectors, with the goal of providing a new and novel approach to high resolution PET for small animal imaging.

N. N. Shehad, C. S. Martin, and J. L. Lacy are with Proportional Technologies, Inc. 8022 El Rio St., Houston, TX 77054, Tel: 713-747-7324, E-mail: nshehad@proportionaltech.com

II. Materials and Methods

A. Detector Construction and Operation

Straw material of 2 mm diameter was fabricated by a commercial vendor using a high speed winding process. The straw shell consisted of a layer of lead foil (0.001Ó0.025 mm thick) sandwiched between layers of thin plastic Þlm (Mylar ®). The inner Mylar layer was copper-coated to provide conductivity for charge collection. Straw material was cut into lengths of 10 cm. Each 10 cm straw incorporated specially designed end Þttings that provided mechanical coupling of the straw to a dual-board end assembly. In addition, each straw featured components on each end called twisters that allowed for anode wire centering.

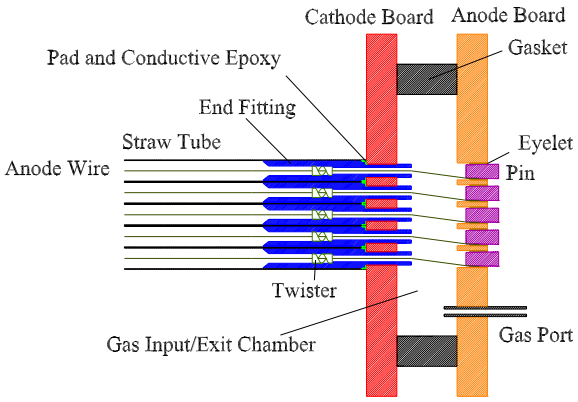

Fig. 1. Side view schematic of module with dual board assembly structure.

A Þberglass module design was developed that incorporated an end assembly structure for gas ßow. It provides a chamber to contain gas with a single entry/exit port and a female connection for the straw end Þttings to plug into. In addition, electrical connections to the anode and the cathode were provided. The design is shown in Figure 1 and was implemented for a 20-straw array. As shown, this assembly structure includes two Þberglass circuit boards, a cathode board and an anode board, spaced by a gas-tight plastic gasket. The straw end Þttings form an open connection to the resulting chamber, which is fed by a single gas input/output port. In this manner, effective gas ßow was achieved. The design was also compatible with efÞcient threading, tensioning, and attachment of the anode wire. Anode wires were held with tension in electrical contact to the anode board using a tapered pin and a brass eyelet.

Rows of straws were assembled using an alignment device and bonding with fast setting cement. These rows were then

0-7803-7636-6/03/$17.00 ©2003 IEEE.

stacked in close packed conÞguration to produce a sturdy 4×5 array module. Single straw detectors were constructed using either 10 μm or 20 μm diameter Stablohm 800 (SO 800) anode wire (California Fine Wire Company). For practical reasons however, in order to minimize risk of breakage, 20 μm wire was used in construction of the straw modules in this Þrst prototype test. Figure 2 shows one of the Þnal modules used for testing.

The optimal operating voltage was empirically determined for each detector conÞguration. Detectors were operated using a Òmagic gasÓmixture consisting of 70% Argon, 29.5% Isobutane, 0.5% Freon 13B1.

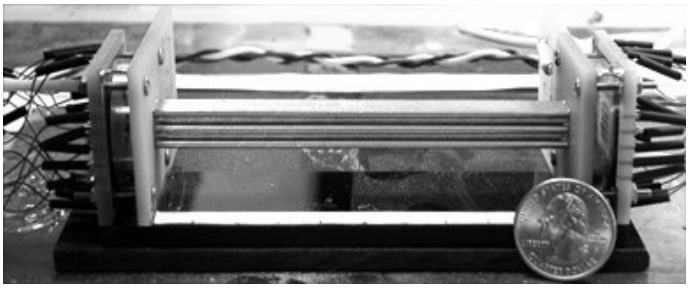

Fig. 2. A 20-straw array with dual-board assembly mounted on each end. Anode and cathode boards can be clearly seen as well as the air tight gasket that allows for gas ßow through the straws. A quarter is pictured to show the relative size of the other components.

B. Resolution Measurements

Longitudinal spatial resolution was assessed for both single straw and module detectors using a charge division method [4]. For each event detected in a straw, a current is injected in the anode wire and splits in proportion to the distance from the end of the straw resulting in a signal on each end (A & B). This current split is determined by the resistance of the anode wire and the longitudinal position of the detected event.

The signals from each end of the detector were fed through anode pulse ampliÞers to an analog-to-digital converter (ADC). Because only one or two straws in a module detect an event at a time, a single summing ampliÞer was used which greatly reduced the electronics requirements of the system. In module operation, in order to minimize the likelihood of signal leakage into adjacent straws, each straw was connected to the summing ampliÞer through a 330 Ω termination resistor at each end.

Two different ADCs were used to digitize detector signals during the course of the work. During preliminary work, an LT344 Lecroy scope was used, which has an 8-bit vertical resolution over the selected input range, a 500 MHz bandwidth, and a 500 MS/s sampling rate. For measurements that required very high ADC accuracy, a second Lecroy scope (LT374L) was used having a vastly improved 4 GS/s sampling rate. Unfortunately, because of budget constraints, the high sampling rate scope could not be used for all experiments even though it yielded much better spatial resolution than its lower sampling rate counterpart.

Once detector signals have been ampliÞed and digitized they are processed in software through a charge integration and charge division technique. The pulse output on each end of the straw is integrated to calculate charge (A & B) and then the ratio A/(A + B) is taken to Þnd the longitudinal position of the event along the length of the straw. This position is then histogrammed.

Intrinsic spatial resolution was measured using a narrowly collimated single photon-emitting source (Tc-99m). This low energy source is detected with very low efÞciency, but it has been previously shown that the spatial response to such a source is indistinguishable from that for 511 keV [3]. The source was collimated with a lead shield such that radiation was incident over a longitudinal section of 0.5 to 1.5 mm in length, placing a lower limit on the longitudinal resolution measurable with this experimental design.

The linearity of longitudinal position measurement was also evaluated by sequentially positioning the collimated source at 1 cm intervals along the length of the straw.

C. Straw Decoding Techniques

In order to achieve 3D PET, an effective method for decoding which straw in an array detected an event is essential. Delay lines offered an attractive approach because signals from several inputs can be distinguished based on time of signal arrival. Decoding techniques based on both cathode and anode readout were considered. Since the anode signal was already being used for longitudinal position measurement, cathode readout is a natural choice for decoding straw identity. Inherent drawbacks to this scheme are that it requires expensive high voltage isolation resistors for each straw and that individual cathode signals must be isolated, which complicates the mechanical design. Also, connecting cathodes together offers an important advantage, because it permits simpler module construction and triggering on the cathode signal. Therefore, decoding based on the cathode signal was rejected.

Instead, an anode technique based on row-column readout was developed. This readout system is depicted in Figure 3. One end of the module consisted of U-connections, where each pair of adjacent strawsÕanodes were connected together, so

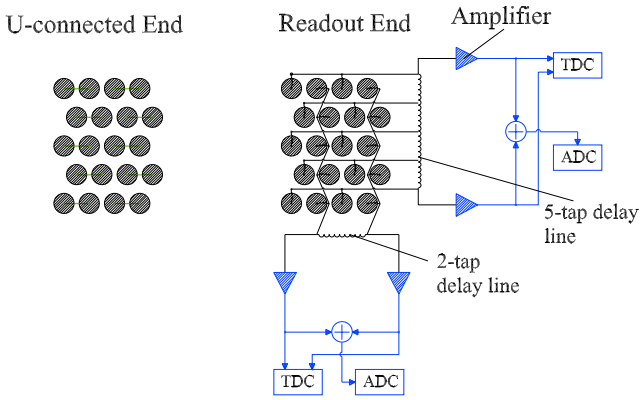

Fig. 3. Experimental readout system with U-connection and delay line encoding. (a) *left*, Adjacent straws are connected at one end to form a U-connection, (b) *right*, Delay line decoding setup for 4 x 5 straw array.

that all readout electronics could be placed on the other end (see Figure 3(a)). This scheme also reduced the number of taps needed on the delay line. Thus, although the straw array is actually a 5x4 row-column matrix, it was read out as a 5x2 matrix of 20 cm ÒeffectiveÓ, U-connected straws, which had both readout ends on the same side of the module.

The ÒeffectiveÓ strawsÓ were connected together through resistors along rows on one end and along columns on the other end (see Figure 3(b)). Each row was connected to a tap in a 5-tap delay line (1 ns/tap), and each column was connected to a tap in a 2-tap delay line (1 ns/tap). Since each tap delays the signal by a Þxed time, the difference in time of arrival at each end of the delay line indicated which row or column contained the active straw. Events were histogrammed based on the differences in arrival times, and a count proÞle was generated for each delay line. For each delay line, the outputs from both ends of the delay line were also summed together to give ÕAÖ and ÕBÖ. Thus, spatial resolution was measured as before using the A/(A+B) charge division technique. Signals were digitized at a sampling rate of 4 GS/sec.

D. Coincidence and Sensitivity

Coincidence detection of a positron source was assessed using two 20-straw arrays placed 50 cm apart with a 200 μCi Na-22 line source (25 mm long) positioned vertically half-way in between the two detectors (Figure 4). When an event was detected in both detectors within a 10 ns window, the event was considered a coincidence event and stored in the computer. A simple reconstruction was then accomplished by drawing all of the lines of response and histogramming their intersection coordinates with the center line containing the source.

Sensitivity of this two-module system was also measured utilizing this same detector conÞguration and time resolution was measured using simple leading edge signal timing between module outputs.

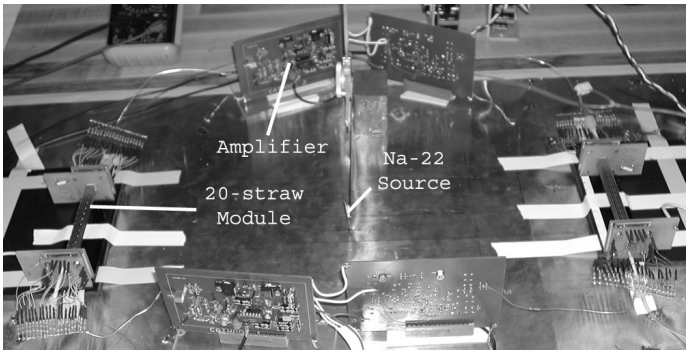

Fig. 4. Experimental setup used for coincidence detection of Na-22 line source. The paralleling of the 20 anode signals through termination resistors into a single ampliÞer is readily seen. The entire readout was done using 4 ampliÞers seen at the center, whose outputs were digitized using an oscilloscope (Lecroy LT344, 500 MS/s).

III. Detector Performance

A. Resolution Performance

As shown in Figure 5(a), the single straw detector (10 μm wire) produced a resolution of 1.0 $\pm$ 0.06 mm FWHM using the 4 GS/s scope. Highly linear position measurement was also observed (R^2 = 0.9999) using the single straw detector, as shown in a correlation plot between the calibrated raw measurement and the actual position (Figure 5(b)).

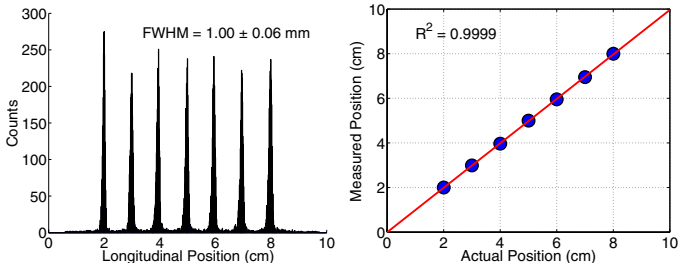

(a) (b)

Fig. 5. (a) Longitudinal resolution measurements from a single 10 cm straw with 10 μm anode wire. The source was sequentially positioned at 1 cm intervals, and 1 mm resolution was observed at all positions. A 4 GS/s ADC was used for digitization. (b) XY plot of calibrated measured position and the actual position.

Resolution worsened somewhat to 1.4 mm with use of the 20 μm wire (Figure 6(a)) due to this wireÕs lower resistance. A 20-straw array produced a resolution of 1.8 mm FWHM (Figure 6(b)), which compares favorably to the single straw result for 20 μm wire. Loss of resolution may result from connection of multiple straws to a common pulse ampliÞer, which has some Þnite input impedance. Nonetheless, this is a rather stunning result demonstrating that a high level of paralleling of readout is possible with accompanying reduction in multiplicity of readout components. AmpliÞer optimization could even further narrow the gap between single straw and module performance.

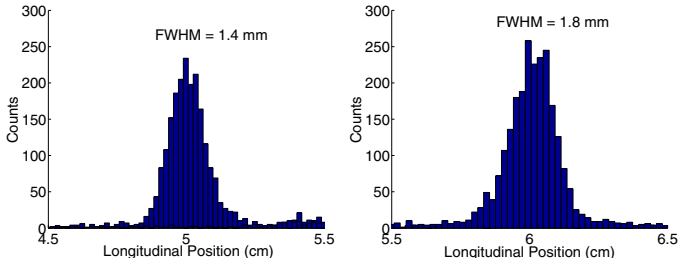

(a) (b)

Fig. 6. Longitudinal resolution measurement from (a) a single 10 cm straw with 20 μm anode wire (b) a 20-straw module with 20 μm anode wire. A 4 GS/s ADC was used for digitization in both measurements.

B. Straw Decoding Results

To evaluate the performance of the straw decoding system proposed, ÒeffectiveÓstraw anodes were connected along rows on one end and along columns on the other end. The count proÞles produced by each delay line are shown in Figure 7. Well-differentiated peaks were observed, supporting the feasibility of this technique to identify which straw is active. Use of delays lines with greater time delay per tap would enable peaks to be even better resolved.

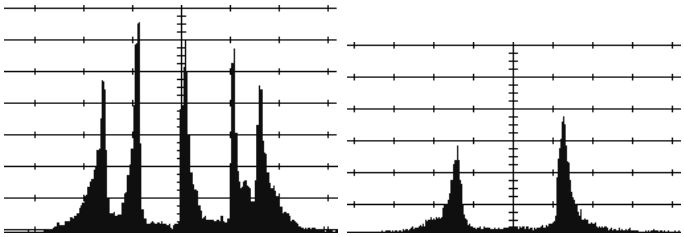

(a) (b)

Fig. 7. (a) Count proÞle produced by 5-tap delay line. The peaks represent events occurring in each of the Þve rows. (b) Count proÞle produced by the 2-tap delay line. The two peaks represent the events occurring in each of the two ÒeffectiveÓcolumns.

Since all anodes were now connected together through delay lines, this raised some concerns regarding degradation of spatial resolution. The success of this straw decoding approach largely relied upon preserving spatial resolution despite introducing the additional decoding electronics. Spatial resolution was measured to determine if the additional straw decoding electronics reduced the overall resolution performance of the system. Figure 8 shows that a spatial resolution of 1.7 mm was achieved which very closely matches and even exceeds that achieved by the module without delay lines, which showed 1.8 mm resolution.

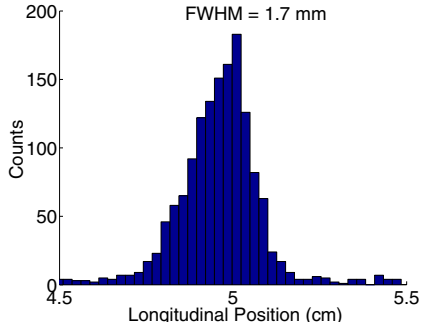

Fig. 8. Resolution of module with 20 μm wire using delay line straw decoding and 4 GS/s digitization

C. Coincidence and Sensitivity Results

Successful coincidence imaging of a line source was accomplished with the straw modules. Using the pairs of longitudinal coordinates measured by the two detectors, a simple 2-D reconstruction was performed to produce the line of response image shown in Figure 9(a). A reconstructed spatial resolution of 2.9 mm was produced (Figure 9(b)). This result was obtained using the lower sampling rate 500 MS/s scope, which yielded a single module resolution of 2.5 mm. Given the very rough reconstruction method, this reconstructed resolution compares well with previous results from the single module experiments. Furthermore, it has been shown that superior resolution can be obtained using a smaller diameter (10 μm) anode wire. Thus, substantial improvement in reconstructed resolution is highly likely.

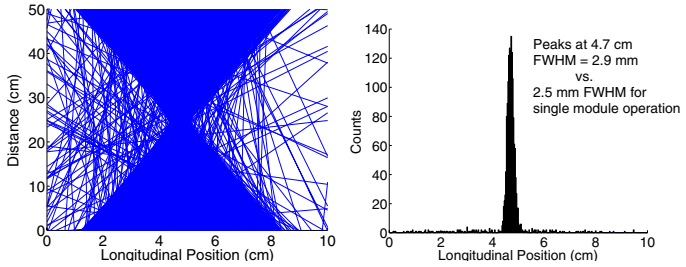

(a) (b)

Fig. 9. (a) Line of response image based on longitudinal position measurements obtained from coincidence operation of two 20-straw modules. Digitization was performed using a 500 MS/s scope. (b) Reconstructed spatial resolution obtained from the coincidence experiment in (a).

Experimental coincident sensitivity (29.5 cps/mCi) was found to agree very well with the theoretically predicted value of 31.8 cps/mCi. We consider this exceptional agreement since small loss of efÞciency is expected due to Þnite length of the line source and from potential Þne source positioning errors in the vertical direction. Timing resolution for two 20-straw detector modules was 8.8 ns FWHM (Figure 10). Previous results with the same gas mixture and 5 mm straws gave 21 ns FWHM [3]. Thus as expected time resolution scales with diameter of the straw indicating that if the straw is reduced further a corresponding time resolution improvement is expected.

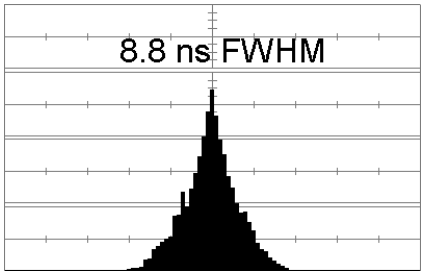

Fig. 10. Histogram of absolute time differences observed between coincidence events of 2 20-straw modules. Timing resolution of 8.8 ns FWHM was observed.

IV. Conclusion

In summary, testing of a single 2 mm straw with a 10 μm Stablohm 800 anode wire yielded intrinsic longitudinal spatial resolution of 1 mm FWHM. Furthermore, resolution showed very modest degradation due to operation of straws in a close-packed array, essentially no loss of performance was observed due to addition of readout electronics (e.g. delay lines). Even when using suboptimal 20 μm anode wire, axial resolution of 1.7 mm was attained in module operation. Preliminary testing of a straw decoding technique was also highly successful and supports the feasibility of accurate position measurement, with very few electronic components. The good agreement between theoretical and experimental sensitivities and excellent timing resolution results confirm theoretical predictions of exceptional PET imaging characteristics. In addition, as previously described, low-cost structural components and efficient techniques for manufacture of the modules were developed, making the overall design well-suited for implementation in a full scale imaging system. Overall, the work was highly successful, accomplishing all goals originally set out, and demonstrates that 2 mm diameter LWS detectors can provide a practical, low-cost alternative to crystal detectors for use in ultra high resolution PET applications, namely small animal imaging and in fact provide significantly improved imaging performance.

References

[1] A. F. Chatziioannou, S. R. Cherry, Y. Shao, R. W. Silverman, K. Meadors, T. H. Farquhar, M. Pedarsani, and M. E. Phelps, "Performance evaluation of MicroPET: a high-resolution Lutetium Oxyorthosilicate PET scanner for animal imaging," *J Nucl Med*, vol. 40, no. 7, pp. 1164–1175, 1999.

[2] M. V. Green, J. Seidel, J. J. Vaquero, E. Jagoda, I. Lee, and W. C. Eckelman, "High resolution PET, SPECT and projection imaging in small animals," *Comput Med Imaging Graph*, vol. 25, no. 2, pp. 79–86, 2001.

[3] J. Lacy, C. Martin, and L. Armendarez, "High sensitivity, low cost PET using lead-walled straw detectors," *Nucl. Instrum. Meth.*, vol. A471, pp. 88–93, 2001.

[4] V. Radeka and P. Rehak, "Charge dividing mechanism on resistive electrode in position-sensitive detectors," *IEEE Trans. Nuc. Sci.*, vol. NS-26, no. 1, pp. 73–80, 1979.